SCIENTIFIC REPORTS

OPEN

SUBJECT AREAS:
CANCER IMAGING
APPLIED PHYSICS

Received
22 January 2014

Accepted
13 February 2014

Published
19 March 2014

Correspondence and requests for materials should be addressed to C.D.L. (clogsdon@mdanderson.org)

Targeting Pancreatic Ductal Adenocarcinoma Acidic Microenvironment

Zobeida Cruz-Monserrate[1], Christina L. Roland[2], Defeng Deng[1], Thiruvengadam Arumugam[1], Anna Moshnikova[3], Oleg A. Andreev[3], Yana K. Reshetnyak[3] & Craig D. Logsdon[1,4]

[1]Department of Cancer Biology, University of Texas, M. D. Anderson Cancer Center, Houston, TX, USA, [2]Department of Surgical Oncology, University of Texas, M. D. Anderson Cancer Center, Houston, TX, USA, [3]Physics Department, University of Rhode Island, Kingston, RI, USA, [4]Department of GI Medical Oncology, University of Texas, M. D. Anderson Cancer Center, Houston, TX, USA.

Pancreatic ductal adenocarcinoma (PDAC) is the fourth leading cause of cancer death in the USA, accounting for ~40,000 deaths annually. The dismal prognosis for PDAC is largely due to its late diagnosis. Currently, the most sensitive diagnosis of PDAC requires invasive procedures, such as endoscopic ultrasonography, which has inherent risks and accuracy that is highly operator dependent. Here we took advantage of a general characteristic of solid tumors, the acidic microenvironment that is generated as a by-product of metabolism, to develop a novel approach of using pH (Low) Insertion Peptides (pHLIPs) for imaging of PDAC. We show that fluorescently labeled pHLIPs can localize and specifically detect PDAC in human xenografts as well as PDAC and PanIN lesions in genetically engineered mouse models. This novel approach may improve detection, differential diagnosis and staging of PDAC.

Approximately 45,000 Americans are diagnosed with pancreatic ductal adenocarcinoma (PDAC) each year and the incidences of PDAC are rising[1]. Unfortunately, there has been little progress in the outcomes of patients with PDAC since the 1970s. Surgical resection is the mainstay of therapy; however, only 20% of patients are eligible for resection due to the presence of advanced disease at the time of diagnosis[2]. The lack of specific symptoms (due to the physical position of the organ), and the lack of sensitive and specific biomarkers, make obtaining a diagnosis difficult at an early stage[3]. For these reasons, there is an urgent need for tools to aid in the early and specific detection of PDAC prior to the development of micro-metastatic disease. To date the most commonly used modalities for diagnosing PDAC, including computed tomography (CT), magnetic resonance imaging (MRI) and endoscopic ultrasonography (EUS), are unable to detect early lesions and are mainly used for disease staging[3,4].

In the current study, instead of employing a traditional molecular targeting strategy based on imaging of a single biomarker protein overexpressed in a subset of cancer cells, we evaluated a more general approach for targeting: the acidity of the tumor microenvironment. Acidosis is generated as a by-product of cancer cell metabolism and it is correlated with tumor development and progression[5–7]. Imaging the acidic microenvironment avoids the common problem of heterogeneity of protein biomarkers, which limits the usefulness of agents directed to specific cell surface markers[8,9]. We employed recently developed pH-sensitive probes, pH (low) insertion peptides (pHLIPs®) to image PDAC in mice. The pHLIPs are water-soluble membrane peptides, which insert into the lipid bilayer of membranes and form transmembrane helix only within an acidic extracellular microenvironment, such as that found in tumors[10–13]. We show that the fluorescently-labeled pHLIP probes detected PDAC tumors, metastasis and PanIN lesions in preclinical mouse models of PDAC. The obtained data provide critical proof of principle supporting further development of this novel approach, which will ultimately lead to a clinical breakthrough for early detection and diagnosis of PDAC.

Results

The goal of our study is to demonstrate the feasibility of targeting the extracellular acidity for imaging PDAC in different tumor models. To achieve this goal we used pH-sensitive WT-pHLIP peptide and its control, 2K-WT-pHLIP (Table 1) which have been well validated in other tumor models[13–17]. The protonatable Asp residues in transmembrane (TM) part of the 2K-WT-pHLIP are replaced by the positively charged non-protonatable Lys

Table 1 | Sequences of pHLIP peptides used in the study. The transmembrane (TM) sequences of the peptides are shown in bold

Variant ID	Sequence
WT-pHLIP	ACEQNPIY **WARYADWLFTTPLLLLDLALLV** DADEG
2K-WT-pHLIP	ACEQNPIY **WARYAKWLFTTPLLLLKLALLV** DADEG
Var3-pHLIP	ACDDQNP **WRAYLDLLFPTDTLLLDLLW**
Var7-pHLIP	ACEEQNP **WARYLEWLFPTETLLLEL**

residues, which reduces pH-dependent ability of the 2K-WT-pHLIP to insert into membrane. In addition, we investigated targeting of PDAC with pHLIP variants, Var3 and Var7 (see Table 1) as they have recently been identified as novel variants that are suited very well for imaging of acidic tumors[12]. All peptides contain single Cys residue at the non-inserting into membrane termini (Table 1), which was conjugated with Alexa546 or Alexa647 fluorescent dyes. The constructs were purified and used in *in vivo* and *ex vivo* fluorescent studies.

pHLIP targets PDAC and peritoneal metastasis in human pancreatic cancer xenografts. To test if tumor acidity could serve to detect primary tumors, we used an orthotopic mouse model of PDAC in which human PDAC cells tagged with luciferase were injected directly into the pancreas and tumor growth was monitored weekly via bio-luminescence imaging. Once tumors were formed (Figure 1A) animals were injected with 40 μM of WT-pHLIP via tail vein. We compared whole body fluorescence imaging signals of mice with tumors injected with probe (tumor +WT-pHLIP), with

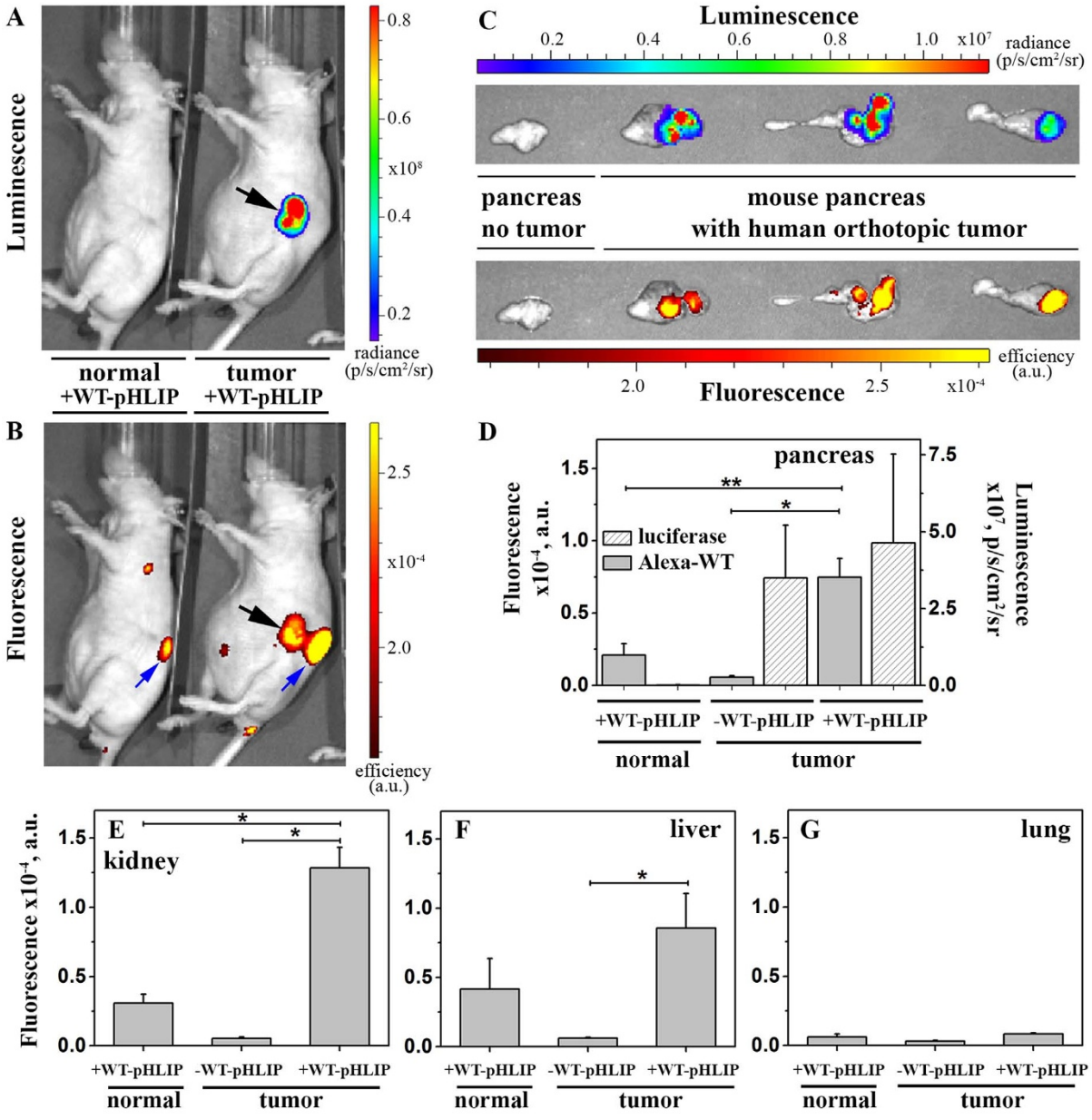

Figure 1 | pH-sensitive probes efficiently detect human pancreatic cancer xenografts. Representative *in vivo* bioluminescent (A) and fluorescent (B) images of athymic nude mice without tumor (normal; n = 5; left) and with tumor (orthotopic model of PDAC with luciferase-labeled Capan-2 cells; n = 5) injected with 40 μM of Alexa647-WT-pHLIP in 100 μl of PBS. Tumor and kidneys are indicated by black and blue arrows, respectively. Representative *ex vivo* images of normal pancreas and PDAC from mice injected with Alexa647-WT-pHLIP (C). *Ex vivo* bioluminescent and fluorescence signal quantification of pancreas (n = 5 per group) (D) and fluorescence signal quantification of liver, kidney and lung (E–G). Values are means ± SEM, *p = 0.0167, **p = 0.0025.

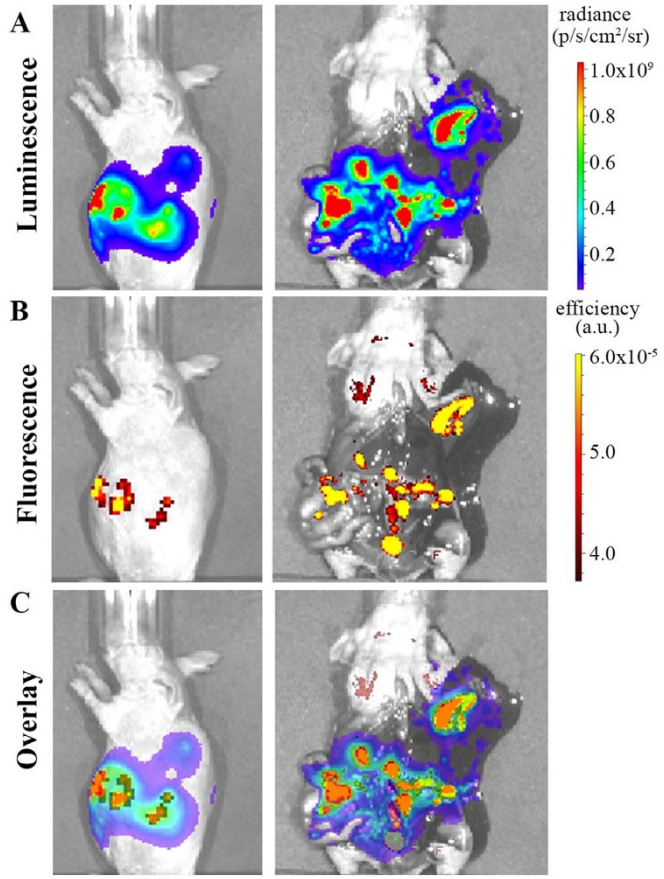

Figure 2 | pH-sensitive probes detect primary tumors and metastasis in human pancreatic cancer xenografts. Orthotopic model of PDAC with luciferase-labeled Capan-2 cells injected with 40 μM of Alexa647-WT-pHLIP in 100 μl of PBS (+pHLIP; n = 5) Bioluminescent signal indicating tumor growth and metastasis (A) co-localizes with the fluorescent signal demonstrating pH-dependent targeting by Alexa647-WT-pHLIP (B). The overlay of the signals are shown on (C).

mice containing tumors but not injected with probe (tumor –WT-pHLIP) and control mice without tumors injected with probe (normal +WT-pHLIP; Figure 1). We found that the fluorescence emitted after 24 hrs of injection was localized mostly in the kidney and PDAC (Figure 1B). The time point of 24 hrs post-injection was selected based on the results of our previous findings, which indicate that the initial blood uptake is typically 45% ID/g decreasing steadily to 1–3% ID/g at 24 hrs post injection[14,15]. The metabolism data showed that WT-pHLIP consisting all of D-amino acids remains intact in the blood of living rats up to at least 1 hr post injection, which is enough time frame for tumor targeting. The slow clearance profile is due to the interaction (no insertion) of pHLIP with cellular membranes at neutral pH. The constructs are retained in tumors for at least 2 days when pHLIP is inserted into cellular membranes at low extracellular pH.

Ex-vivo examination of the pancreas from mice with and without tumors indicates the WT-pHLIP probe specifically targets to the tumor-bearing pancreas, but not normal pancreas (Figure 1C, D). The fluorescent signal in pancreases of mice bearing tumor was 13.6 times higher ($p = 0.0025$) than fluorescence in normal pancreas (Supplementary Table 1). Signals from liver, kidney, and lung were also quantified (Figure 1E–G and Supplementary Table 1). Interestingly, the signal in the kidney at 24 hrs after WT-pHLIP administration was significantly higher in mice bearing tumors than in non-bearing tumor mice (Figure 1E). Moreover, to determine if acidosis could be used as a marker to detect metastases, mice with detectable metastasis via luminescence signal (Figure 2A) were injected with fluorescently labeled WT-pHLIP. After 24 hrs of probe injection, the fluorescence of WT-pHLIP from primary tumor and all peritoneal metastasis were co-localized with the luminescence signal (Figure 2).

pHLIPs act in a pH dependent manner to detect PDAC and metastasis in genetically engineered mouse models (GEMMs) and early PanIN lesions. To verify our findings of acidosis as a marker for imaging primary PDAC and metastasis in an autochthonous model of PDAC, the ability of WT-pHLIP probe to image tumors developed in well-established GEMMs was tested[18,19]. Similar to the orthotopic model, we found that WT-pHLIP targets PDAC and liver metastasis (Figure 3A) in a GEMM, and demonstrates the strongest signal compared to other organs (Figure 3B–E and Supplementary Table 2). The fluorescent signal in pancreases of mice bearing tumor was 17.6 times higher ($p = 0.0043$) than fluorescence in normal pancreas. Moreover, to test if PDAC and metastasis pHLIP targeting was pH dependent, the animals were injected with the control pH-insensitive probe, 2K-WT-pHLIP. Indeed the fluorescence signals detected in the mouse tissues are pH-dependent as the signals from PDAC and kidney are significantly reduced in mice injected with 2K-WT-pHLIP compared to WT-pHLIP (Figure 3B–F and Supplementary Table 2). Similar to the orthotopic model, the signal in the kidney at 24 hrs after WT-pHLIP administration was significantly higher in tumor-bearing mice than in non-bearing tumor mice (Figure 3C). Histologic evaluation of pancreas from PDAC mice injected with WT-pHLIP show a significant increase in the fluorescence compared to normal pancreas injected with WT-pHLIP (Figure 4).

The ability to detect PDAC at an early stage is of great clinical necessity and significance. Therefore, we tested the ability of WT-pHLIP to target pre-malignant and early stage PDAC by imaging mice with PanIN lesions. The fluorescent signal from the mice with PDAC was the strongest compared to mice with pancreas containing early PanIN lesions (Figure 5A–B). At the same time, we observed a statistically significant 9.2 times increase ($p = 0.0357$) in fluorescence signal from the mice pancreas containing PanIN lesions compared to control mice pancreas (Figure 5 and Supplementary Table 3).

Finally, we tested performance of recently identified new pHLIP variants such as Var3 and Var7. Targeting for both pHLIP variants was pH-dependent (Figure 6 and Supplementary Table 4) similar to WT-pHLIP. The fluorescent signal in pancreases targeted by Var3 and Var7 of mice bearing tumor was 12.4 ($p = 0.0003$) and 22.8 ($p = 0.0043$) times higher than fluorescence in normal pancreas, respectively.

Discussion

Targeting and imaging of tumor acidity is an attractive strategy, given that acidity is a general property of the tumor microenvironment that is less likely to be subject to tumor resistance and selection. Acidity as a universal marker for tumor targeting is associated with tumor development due to a combination of factors, like hypoxia, glucose uptake and carbonic anhydrase activity[5–7]. Rapid cell growth and an inadequate blood supply produce hypoxic conditions that cause a partial use of glycolysis in tumor cells, resulting in acidification of the cytosol, to which the cell adjusts by pumping protons into the external environment. However, hypoxia and low blood supply are not the only mechanisms responsible for the development of an acidic environment within solid tumors[20]. Malignant cancers have an elevated glucose uptake even under normal oxygen conditions, overwhelming the mitochondrial capacity and using glycolysis for the overflow. This condition is known as "aerobic glycolysis" or the Warburg effect[21]. Cells exhibiting a Warburg effect catabolize glucose at a high rate[6,22], and the use of glycolysis results in much higher level of protons and lactic acid, which are pumped across the cell plasma

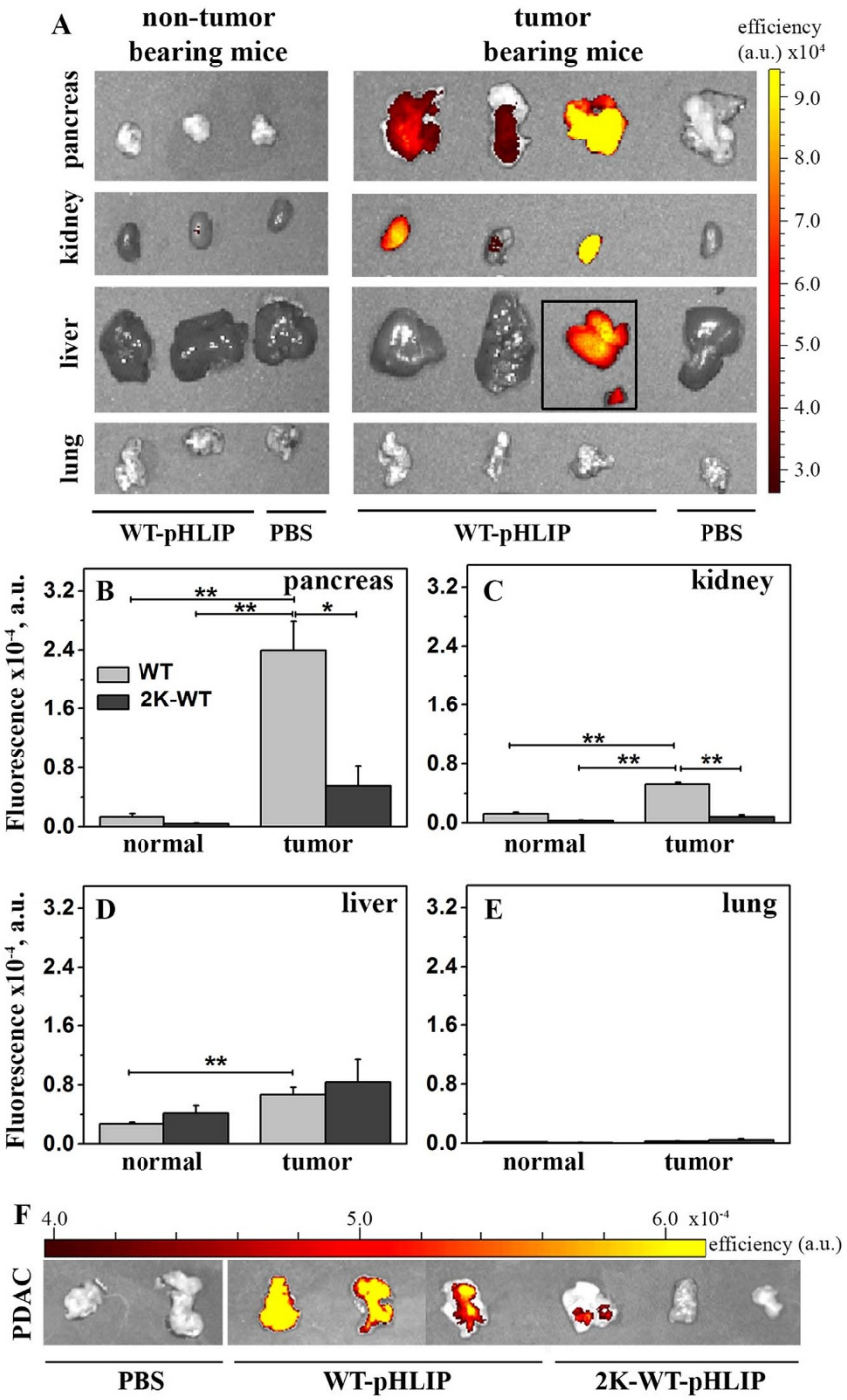

Figure 3 | Probes act in a pH dependent manner to detect PDAC and metastasis in GEMMs. GEMM with normal pancreas (non-tumor bearing mice; n = 10) or PDAC (tumor bearing mice; n = 10) were injected via the tail vein with 40 μM of Alexa546-WT-pHLIP in 100 μl of PBS (n = 5) or with 40 μM of Alexa546-2K-WT-pHLIP (peptide sequence modified to be less sensitive to pH) in 100 μl of PBS (n = 5). (A) Representative *ex vivo* fluorescence images of pancreas, kidney, liver and lung of non-tumor bearing mice (left) and tumor bearing mice (right) 24 hrs after Alexa546-WT-pHLIP injection. Liver metastases were visualized in some mice (square) which correlated with an increase in fluorescent signal. (B–E) *Ex vivo* fluorescence quantification of non-tumor bearing mice (n = 10) and tumor bearing mice (n = 10) injected with Alexa546-WT-pHLIP or Alexa546-2K-WT-pHLIP. (F) Comparison of tumor targeting by Alexa546-WT-pHLIP and Alexa546-2K-WT-pHLIP (control). Values are means ± SEM, *p = 0.0159, **p = 0.0043.

membrane into the extracellular space, where they accumulate in poorly perfused regions[23–25]. In addition to the lactic acid-output, expression of carbonic anhydrases 9/12 on the tumor cell surface catalyzes the extracellular trapping of acid by hydrating cell-generated CO_2 into HCO_3^- and H^+[26,27]. These mechanisms in combination create an acidic extracellular milieu favoring tumor growth, invasion and development. Moreover, the extracellular pH of solid tumors plays a role in almost all steps of metastasis, and acidic tumors become highly aggressive and metastatic[28].

The Warburg effect and altered metabolic pathways has been reported in PDAC supporting the targeting of acidosis for this tumors[29–31]. Therefore, in present study, we used pH-sensitive

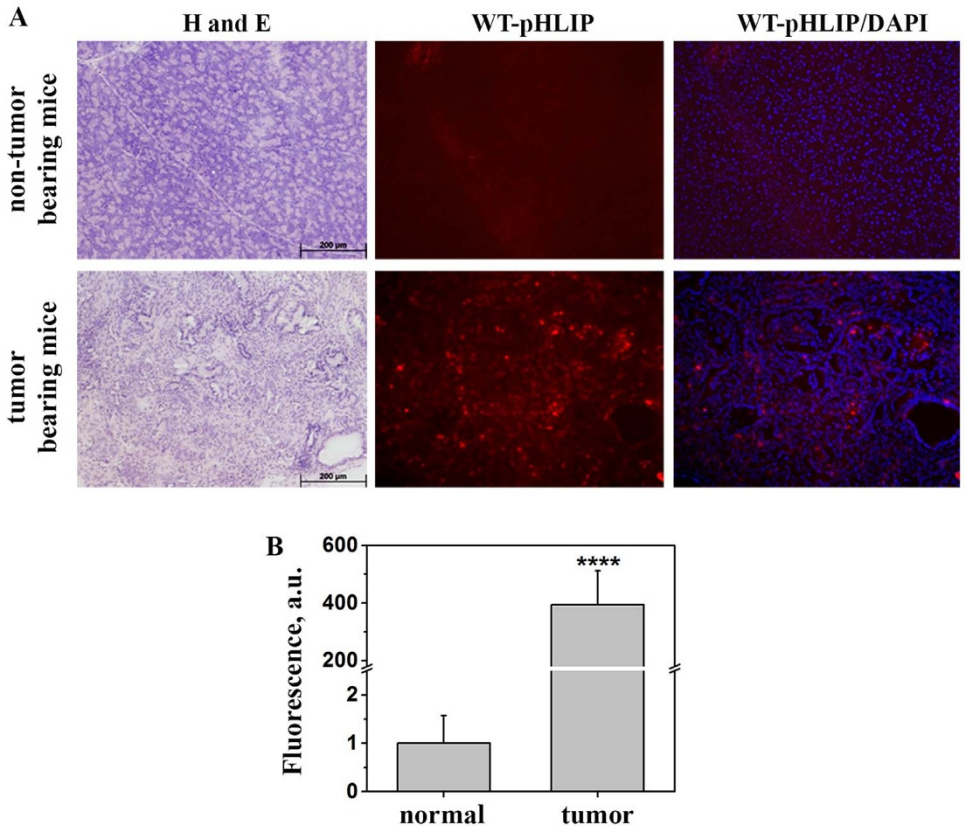

Figure 4 | pH-sensitive probes localize to PDAC and not normal pancreas in GEMMs. (A) H & E, fluorescence of Alexa647 (WT-pHLIP) and DAPI (nuclei) signal of non-tumor bearing mice (top) and tumor bearing mice (bottom) treated with 40 μM of Alexa647-WT-pHLIP in 100 μl of PBS (n = 5). (B) Quantification of fluorescence signal relative to nuclei staining. Values are means ± SEM, ****$p < 0.0001$.

pHLIP probes labeled with fluorescent Alexa dyes to evaluate their ability to detect PDAC. We have shown that WT-pHLIP targets primary tumor, peritoneal and liver metastasis with high accuracy. The fluorescent signal in pancreases of mice bearing tumor is 13–17 times higher than the fluorescence in normal pancreas injected with pHLIP. The targeting is pH-dependent, as a pH-insensitive control pHLIP probe (2K-WT-pHLIP) shows significantly less accumulation in acidic tumors and kidney. Thus, pHLIP probes demonstrate high specificity and sensitivity in targeting of pancreatic tumors. An interesting finding of our study, which might have important clinical relevance, is an enhanced fluorescence signal in the kidneys of tumor bearing animals injected with pHLIP compared to non-tumor bearing animals. It could be associated with the elevated acidity in the kidneys of tumor bearing mice and might be used to monitor disease in urine with clinical significance. Another important finding is the ability of pHLIP to target PDAC in its early stages (PanIN lesions). Importantly, normal pancreas does not accumulate WT-pHLIP, making it a sensitive and specific test for the diagnosis of early stage PDAC. These are significant findings for the development of imaging protocols to detect early neoplastic transformations from normal pancreas in order to increase the odds of detecting this deadly disease at an early stage. In addition to WT-pHLIP, we tested two other pHLIP variants: Var3 and Var7. The latest one, Var7 shows fast blood clearance in xenograft models of lung and cervical cancer[12] suggesting that it may be the best probe for PET (positron emission tomography) and SPECT (single photon emission computed tomography) imaging. Indeed, we observed 23 times increase of fluorescence signal in pancreases of mice bearing tumor compared to the fluorescence in pancreas of normal mice injected with Var7.

In summary, this work provides fundamental preclinical evidence using various mouse models that targeting of tumor acidity in pancreas by the pH-sensitive pHLIP probes might be useful for the clinical detection of PDAC. It opens an opportunity for the development of novel imaging clinical protocols to improve detection, narrow the differential diagnosis and improve staging of PDAC. Other use of this probe for surveillance of PDAC will help improve survival as it will be able to detect most tumors in a resectable stage.

Methods

Conjugation of pHLIP Variants with Fluorescent Dyes. pHLIP variants were prepared by solid-phase peptide synthesis using Fmoc (9-fluorenylmethyloxycarbonyl) chemistry and purified by reverse phase chromatography at the W.M. Keck Foundation Biotechnology Resource Laboratory at Yale. Each pHLIP variant was conjugated with AlexaFluor®546 and AlexaFluor®647 C5-maleimide in DMSO at a ratio of 1 : 1.2 of dye : peptide and incubated at room temperature for 4–8 hours. The reaction progress was monitored by reverse phase HPLC. The products were isolated via HPLC. Peak identity was confirmed by SELDI-TOF mass spectrometry and analytical HPLC. The concentrations of the conjugated peptides were determined by absorbance (for Alexa546: $\varepsilon = 93{,}000\ M^{-1}cm^{-1}$; and for Alexa647: $\varepsilon = 265{,}000\ M^{-1}cm^{-1}$).

Cell Lines. An established pancreatic cancer cell line (Capan- 2) was obtained from the American Type Culture Collection (ATCC, Manassas, VA). Cells were routinely cultured in recommended media. All cells were maintained at 37°C in a humidified atmosphere of 5% CO2.

Immunocytochemistry. Frozen tissue slides were covered using VECTASHIELD mounting medium (Vector laboratories, Burlingame, CA). Sections were examined on a Zeiss Axioplan2 microscope and images captured with a Hamamatsu ORCA-ER camera with Image-Pro Plus software (Media Cybernetics, Rockville, MD) and analyzed using Simple PCI software (Hamamatsu Corporation, Sewickley, PA).

Animal models. To assess if pHLIP can serve as a biomarker for *in vivo* imaging, studies were performed in human pancreatic cancer xenografts in immunodeficient (acquired from The National Cancer Institute with age ranging from 5–6 weeks old) and transgenic mice. Animals were housed at the MD Anderson Cancer Center animal facility. All animal procedures were performed in accordance with the MD Anderson Cancer Center (Houston, TX) institutional guidelines using an approved animal protocol by the Institutional Animal Care and Use Committees of the

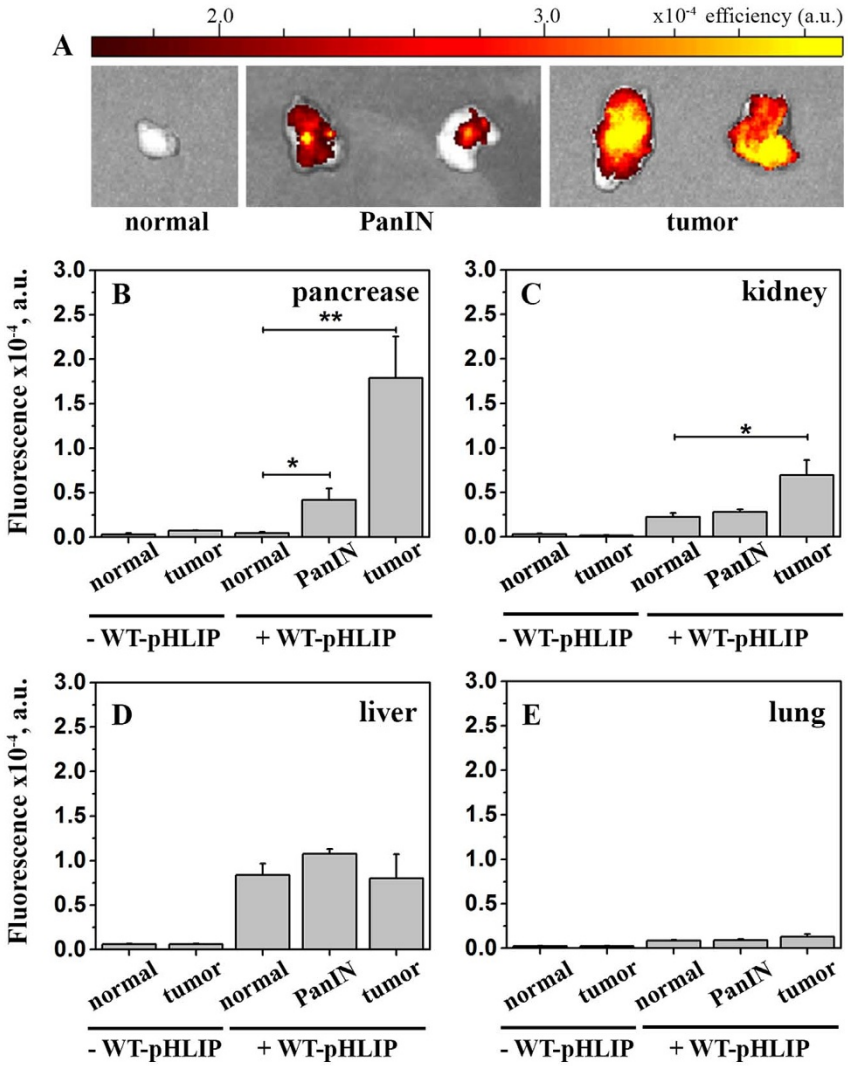

Figure 5 | pHLIP can detect early PanIN lesions and tumors in GEMMs. Representative *ex vivo* fluorescence images of pancreas (A) and fluorescence quantification of pancreas (B), kidney (C), liver (D) and lung (E) from non-tumor bearing mice (n = 10), tumor bearing mice (n = 10), mice containing PanIN lesions (n = 5) and mice with pancreatitis (n = 5) which were injected with 40 μM of Alexa647-WT-pHLIP in 100 μl of PBS or 100 μl of PBS. Values are means ± SEM, *p < 0.0357, **p = 0.0016.

University of Texas MD Anderson Cancer Center. Mice used for optical imaging studies were fed with chlorophyll-free diet.

Genetic PanINs and PDAC mouse models were developed by crossing LSL-KRas^{G12D} mice[32] with floxed p53 mice[33] and pancreatic specific cre (Pdx-1-Cre) mice[34] to yield mice which possessed conditional p53 deletion and endogenous levels of mutant KRas^{G12D} [18]. PDAC in this mice developed in 6–8 weeks after birth[35]. Littermates without PDAC served as controls. Moreover, LSL-KRas^{G12D} mice[32] were cross with elastase (Ela) tamoxifen-regulated CreERT (Ela-CreERT) as described previously[36] and fed a high-fat diet for 30 days to induce PanIN 1 lesions as previously describe[19]. LSL-KRas^{G12D}, p53 floxed, and Pdx-1-Cre genetic mice were obtained from the Mouse Models for Human Cancer Consortium Repository (Rockville, MD).

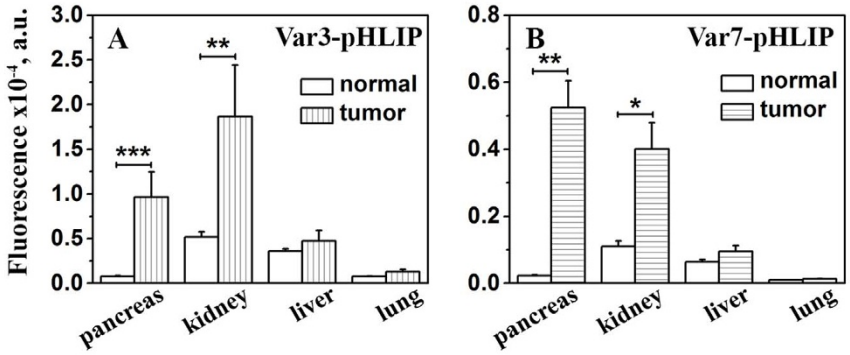

Figure 6 | pHLIP variants can detect PDAC efficiently in GEMMs. *Ex vivo* fluorescence quantification of pancreas, kidney, liver and lung from non-tumor bearing mice (n = 10) and tumor bearing mice (n = 10) injected with 40 μM of Alexa647-Var3-pHLIP (A) and Alexa546-Var7-pHLIP (B) in 100 μl of PBS. Values are means ± SEM, *p = 0.02, **p < 0.0043, ***p = 0.0003.

To establish orthotopic tumors, mice were anesthetized with a single intraperitoneal injection of ketamine (100 mg/kg) and xylazine (10 mg/kg) and then the pancreas was exposed through a left abdominal incision (laparotomy). Sub-confluent Capan-2 cells (ATCC, Manassas, VA) labeled with firefly luciferase as per[37] were detached with 0.25% trypsin-EDTA and cell viability was assessed by trypan blue exclusion. Capan-2 cells are one of the few PDAC cell lines that form a prominent stromal reaction mimicking the human tumor. Cells (1.8×10^5) were resuspended in 50 μL of Hanks Balanced Salt Solution (HBSS) and directly injected into the pancreas (caudal). After tumor implantation, the pancreas was carefully returned to the peritoneal cavity and the abdomen was closed. Tumor growth was assessed every week by bioluminescence imaging for 8 weeks using a cryogenically cooled imaging system coupled to a data acquisition computer running Living Image 4.3.1 software (Xenogen/Caliper, Alameda, CA). Before imaging, animals were injected subcutaneously with 40 mg/mL of luciferin potassium salt in PBS at a dose of 150 mg/kg body weight. Signal intensity was quantified as the sum of all detected photons within the region of interest per second. Two months after tumor implantation, pH-sensitive and control probes were injected via tail vein and imaged 24 hrs after injection. Tissues were also fixed with formaldehyde or snap frozen in liquid nitrogen and examined histologically.

***In vivo* and *ex vivo* Imaging.** Animals were injected with a single dose of the fluorescence pH-sensitive and controls probes (40 μM pHLIP/100 μl PBS) or 100 μl PBS (controls without probe) intravenously through tail vein using a 30 gauge syringe needle. After 24 hrs the anesthetized mice were placed in the heated imaging platform of IVIS-Spectrum optical imaging systems (Xenogen/Caliper, Mountain View, CA). White light and near infrared fluorescence (NIRF) images were acquired sequentially using fluorescence filters for Alexa546 and Alexa647. Mice were imaged 24 hrs post probe intravenous injection. Mice were sacrificed and organs/tissues were excised and rinsed with PBS then imaged for their associated NIRF. Fluorescence variations between different organs/tissues were corrected by subtracting the auto-fluorescence signals obtained from imaging organs/tissues of mice without any probe injected. General illumination setting and image acquisition parameters were: epi-illumination; 0.5 sec. exposure time; f/stop = 2; binning (HR) 4; field of view (FOV = 12.9 cm or 6.5 cm width and height). Luminescence each image was defined as photons per second per centimeter squared per steradian ($p/s/cm^2/sr$). Fluorescence contrast, defined as radiance, was quantified using identical size regions of interest (ROI).

Statistical analysis. Data are presented as mean ± SEM. For in vivo studies, we used 5 animals per group ($n = 5$). Statistically significant differences were determined by two-tailed unpaired Student's t-test ($P < 0.05$ was taken as significant). When more than 2 groups were analyzed, ANOVA was used to analyze the data and the Newman–Keuls multiple comparison test was used to check the posttest significance. Statistical significance was defined as $P < 0.05$.

1. Siegel, R., Naishadham, D. & Jemal, A. Cancer statistics, 2012. *CA Cancer J Clin* **62**, 10–29, doi:10.3322/caac.20138 (2012).
2. Yeo, C. J. *et al.* Six hundred fifty consecutive pancreaticoduodenectomies in the 1990s: pathology, complications, and outcomes. *Ann Surg* **226**, 248–257; discussion 257–260 (1997).
3. Kramer-Marek, G., Gore, J. & Korc, M. Molecular imaging in pancreatic cancer - A roadmap for therapeutic decisions. *Cancer Lett* **341**, 132–138, doi:10.1016/j.canlet.2013.08.008 (2013).
4. Collisson, E. & Tempero, M. Blinded by the light: molecular imaging in pancreatic adenocarcinoma. *Clin Cancer Res* **17**, 203–205, doi:10.1158/1078-0432.CCR-10-2825 (2011).
5. Gatenby, R. A. & Gillies, R. J. A microenvironmental model of carcinogenesis. *Nat Rev Cancer* **8**, 56–61, doi:10.1038/nrc2255 (2008).
6. Gillies, R. J., Robey, I. & Gatenby, R. A. Causes and consequences of increased glucose metabolism of cancers. *J Nucl Med* **49 Suppl 2**, 24S–42S, doi:10.2967/jnumed.107.047258 (2008).
7. Wojtkowiak, J. W. *et al.* Chronic autophagy is a cellular adaptation to tumor acidic pH microenvironments. *Cancer Res* **72**, 3938–3947, doi: 10.1158/0008-5472.CAN-11-3881 (2012).
8. De Sousa, E. M. F., Vermeulen, L., Fessler, E. & Medema, J. P. Cancer heterogeneity--a multifaceted view. *EMBO Rep* **14**, 686–695, doi:10.1038/embor.2013.92 (2013).
9. Burrell, R. A., McGranahan, N., Bartek, J. & Swanton, C. The causes and consequences of genetic heterogeneity in cancer evolution. *Nature* **501**, 338–345, doi:10.1038/nature12625 (2013).
10. Andreev, O. A., Engelman, D. M. & Reshetnyak, Y. K. pH-sensitive membrane peptides (pHLIPs) as a novel class of delivery agents. *Mol Membr Biol* **27**, 341–352, doi:10.3109/09687688.2010.509285 (2010).
11. Hunt, J. F., Rath, P., Rothschild, K. J. & Engelman, D. M. Spontaneous, pH-dependent membrane insertion of a transbilayer alpha-helix. *Biochemistry* **36**, 15177–15192, doi:10.1021/bi970147b (1997).
12. Weerakkody, D. *et al.* Family of pH (low) insertion peptides for tumor targeting. *Proc Natl Acad Sci U S A* **110**, 5834–5839, doi:10.1073/pnas.1303708110 (2013).
13. Reshetnyak, Y. K. *et al.* Measuring tumor aggressiveness and targeting metastatic lesions with fluorescent pHLIP. *Mol Imaging Biol* **13**, 1146–1156, doi:10.1007/s11307-010-0457-z (2011).
14. Vavere, A. L. *et al.* A novel technology for the imaging of acidic prostate tumors by positron emission tomography. *Cancer Res* **69**, 4510–4516, doi:10.1158/0008-5472.CAN-08-3781 (2009).
15. Macholl, S. *et al.* In vivo pH imaging with (99 m)Tc-pHLIP. *Mol Imaging Biol* **14**, 725–734, doi:10.1007/s11307-012-0549-z (2012).
16. Andreev, O. A. *et al.* Mechanism and uses of a membrane peptide that targets tumors and other acidic tissues in vivo. *Proc Natl Acad Sci U S A* **104**, 7893–7898, doi: 10.1073/pnas.0702439104 (2007).
17. Daumar, P. *et al.* Efficient (18)F-Labeling of Large 37-Amino-Acid pHLIP Peptide Analogues and Their Biological Evaluation. *Bioconjug Chem* **23**, 1557–1566, doi:10.1021/bc3000222 (2012).
18. Olive, K. P. & Tuveson, D. A. The use of targeted mouse models for preclinical testing of novel cancer therapeutics. *Clin Cancer Res* **12**, 5277–5287, doi:10.1158/1078-0432.CCR-06-0436 (2006).
19. Philip, B. *et al.* A High-Fat Diet Activates Oncogenic Kras and COX2 to Induce Development of Pancreatic Ductal Adenocarcinoma in Mice. *Gastroenterology* **145**, 1449–1458, doi:10.1053/j.gastro.2013.08.018 (2013).
20. Chiche, J., Brahimi-Horn, M. C. & Pouyssegur, J. Tumour hypoxia induces a metabolic shift causing acidosis: a common feature in cancer. *J Cell Mol Med* **14**, 771–794, doi: 10.1111/j.1582-4934.2009.00994.x (2010).
21. Warburg, O., Wind, F. & Negelein, E. The metabolism of tumors in the body. *J Gen Physiol* **8**, 519–530 (1927).
22. Newell, K., Franchi, A., Pouyssegur, J. & Tannock, I. Studies with glycolysis-deficient cells suggest that production of lactic acid is not the only cause of tumor acidity. *Proc Natl Acad Sci U S A* **90**, 1127–1131 (1993).
23. Grillon, E. *et al.* The spatial organization of proton and lactate transport in a rat brain tumor. *PLoS One* **6**, e17416, doi:10.1371/journal.pone.0017416 (2011).
24. Rehncrona, S. Brain acidosis. *Ann Emerg Med* **14**, 770–776, doi:S0196-0644(85)80055-X (1985).
25. Xiong, Z. G., Pignataro, G., Li, M., Chang, S. Y. & Simon, R. P. Acid-sensing ion channels (ASICs) as pharmacological targets for neurodegenerative diseases. *Curr Opin Pharmacol* **8**, 25–32, doi:10.1016/j.coph.2007.09.001 (2008).
26. Swietach, P., Vaughan-Jones, R. D. & Harris, A. L. Regulation of tumor pH and the role of carbonic anhydrase 9. *Cancer Metastasis Rev* **26**, 299–310, doi:10.1007/s10555-007-9064-0 (2007).
27. Ihnatko, R. *et al.* Extracellular acidosis elevates carbonic anhydrase IX in human glioblastoma cells via transcriptional modulation that does not depend on hypoxia. *Int J Oncol* **29**, 1025–1033 (2006).
28. Hashim, A. I., Zhang, X., Wojtkowiak, J. W., Martinez, G. V. & Gillies, R. J. Imaging pH and metastasis. *NMR Biomed* **24**, 582–591, doi:10.1002/nbm.1644 (2011).
29. Zhou, W. *et al.* Proteomic analysis reveals Warburg effect and anomalous metabolism of glutamine in pancreatic cancer cells. *J Proteome Res* **11**, 554–563, doi:10.1021/pr2009274 (2012).
30. Son, J. *et al.* Glutamine supports pancreatic cancer growth through a KRAS-regulated metabolic pathway. *Nature* **496**, 101–105, doi:10.1038/nature12040 (2013).
31. Ying, H. *et al.* Oncogenic Kras maintains pancreatic tumors through regulation of anabolic glucose metabolism. *Cell* **149**, 656–670, doi:10.1016/j.cell.2012.01.058 (2012).
32. Jackson, E. L. *et al.* Analysis of lung tumor initiation and progression using conditional expression of oncogenic K-ras. *Genes Dev* **15**, 3243–3248, doi:10.1101/gad.943001 (2001).
33. Jonkers, J. *et al.* Synergistic tumor suppressor activity of BRCA2 and p53 in a conditional mouse model for breast cancer. *Nat Genet* **29**, 418–425, doi:10.1038/ng747 (2001).
34. Hingorani, S. R. *et al.* Preinvasive and invasive ductal pancreatic cancer and its early detection in the mouse. *Cancer Cell* **4**, 437–450, doi:S153561080300309X (2003).
35. Bardeesy, N. *et al.* Both p16(Ink4a) and the p19(Arf)-p53 pathway constrain progression of pancreatic adenocarcinoma in the mouse. *Proc Natl Acad Sci U S A* **103**, 5947–5952, doi:10.1073/pnas.0601273103 (2006).
36. Ji, B. *et al.* Robust acinar cell transgene expression of CreErT via BAC recombineering. *Genesis* **46**, 390–395, doi:10.1002/dvg.20411 (2008).
37. Arumugam, T., Ramachandran, V. & Logsdon, C. D. Effect of cromolyn on S100P interactions with RAGE and pancreatic cancer growth and invasion in mouse models. *J Natl Cancer Inst* **98**, 1806–1818, doi:10.1093/jnci/djj498 (2006).

Acknowledgments

NIH-DK052067 and The Lockton Endowment (to C.D.L.), NIDDK Diversity Supplement DK052067-08 (to C.D.L. for Z.C.-M.), and NIH T32 CA009599 Ruth L. Kirschstein National Research Service Award (to C.L.R.). This research is supported in part by the MD Anderson Cancer Center Support Grant CA016672 (to C.D.L.) and NIH grants CA138468 and GM073857 (to O.A.A. and Y.K.R.). The authors would also like to thank Bincy Philip for technical help and Yan Liu for help with animal genotyping.

Author contributions

Z.C.-M. and C.L.R.: study concept and design, acquisition of data, analysis and interpretation of data, drafting of the manuscript, critical revision of the manuscript for

important intellectual content, and technical support; D.D., T.A. and A.M.: technical and material support; O.A.A., Y.K.R. and C.D.L.: study concept and design, study supervision, analysis and interpretation of data, drafting of the manuscript, critical revision of the manuscript for important intellectual content, obtainment of funding, and technical support.

Additional information

Supplementary information accompanies this paper at http://www.nature.com/scientificreports

Competing financial interests: The authors declare no competing financial interests.

How to cite this article: Cruz-Monserrate, Z. *et al.* Targeting Pancreatic Ductal Adenocarcinoma Acidic Microenvironment. *Sci. Rep.* **4**, 4410; DOI:10.1038/srep04410 (2014).